2

AD

Reports Control Symbol
OSD - 1366

TMR-0012

AD-A252 110

DEVELOPMENT OF MESOSCALE MODEL PERFORMANCE EVALUATION PROGRAMS

April 1992

Teizi Henmi
Roger Vega

Approved for public release; distribution is unlimited.

US ARMY
LABORATORY COMMAND
ATMOSPHERIC SCIENCES LABORATORY
White Sands Missile Range, NM 88002-5501

NOTICES

Disclaimers

The findings in this report are not to be construed as an official Department of the Army position, unless so designated by other authorized documents.

The citation of trade names and names of manufacturers in this report is not to be construed as official Government indorsement or approval of commercial products or services referenced herein.

Destruction Notice

When this document is no longer needed, destroy it by any method that will prevent disclosure of its contents or reconstruction of the document.

REPORT DOCUMENTATION PAGE

Form Approved
OMB No 0704-0188

1. AGENCY USE ONLY *(Leave blank)*

2. REPORT DATE
April 1992

3. REPORT TYPE AND DATES COVERED
Final

4. TITLE AND SUBTITLE
Development of Mesoscale Model Performance Evaluation Programs

5. FUNDING NUMBERS
TA: 62784-AH71-D

6. AUTHOR(S)
Teizi Henmi and Roger Vega

7. PERFORMING ORGANIZATION NAME(S) AND ADDRESS(ES)
U.S. Army Atmospheric Sciences Laboratory
White Sands Missile Range, NM 88002-5501

8. PERFORMING ORGANIZATION REPORT NUMBER
ASL-TMR-0012

9. SPONSORING/MONITORING AGENCY NAME(S) AND ADDRESS(ES)
U.S. Army Laboratory Command
Adelphi, MD 20783-1145

10. SPONSORING/MONITORING AGENCY REPORT NUMBER

11. SUPPLEMENTARY NOTES

12a. DISTRIBUTION/AVAILABILITY STATEMENT
Approved for public release; distribution is unlimited.

12b. DISTRIBUTION CODE

13. ABSTRACT *(Maximum 200 words)*

Computer programs to examine and illustrate the results of mesoscale model simulation and to compare with observation are described. Programs consist of those illustrating horizontal and vertical measurements and temporal distributions of both simulated and observed data. Statistical methods to evaluate model performance are also programmed.

14. SUBJECT TERMS
mesoscale model, model evaluation method

15. NUMBER OF PAGES
37

16. PRICE CODE

17. SECURITY CLASSIFICATION OF REPORT	18. SECURITY CLASSIFICATION OF THIS PAGE	19. SECURITY CLASSIFICATION OF ABSTRACT	20. LIMITATION OF ABSTRACT
Unclassified	Unclassified	Unclassified	SAR

NSN 7540-01-280-5500

Standard Form 298 (Rev. 2-89)
Prescribed by ANSI Std. Z39-18
298-102

CONTENTS

LIST OF FIGURES 4

1. INTRODUCTION 7

2. PROJECT WIND DATA AND MODEL SIMULATION 7

3. DATA INTERPOLATION METHODS 8

   3.1 Upper-Air Data 8

   3.2 Surface Data 9

4. SURFACE METEOROLOGICAL PARAMETERS 9

   4.1 Horizontal Distributions of Gridded Data 9

   4.2 Comparisons of Simulation with Surface Observation 10

5. UPPER-AIR METEOROLOGICAL PARAMETERS 10

   5.1 Vertical Distributions at the Locations of Sounding Stations 10

   5.2 Time-Series at Different Levels 11

6. EVALUATION OF MODEL PERFORMANCE 11

   6.1 Surface Data 12

   6.2 Upper-Air Data 13

7. CONCLUDING REMARKS 14

LITERATURE CITED 37

DISTRIBUTION LIST 39

LIST OF FIGURES

1. Project WIND terrain map, with 400 m height contours.............. 15

2. Interpolation method of vertical data.............................. 16

3. Temperature distribution with 5 °C contours........................ 17

4. Sensible heat flux distribution over terrain data--solid lines for upward flux and broken lines for downward flux................ 18

5. Horizontal wind vector distributions--right side for simulation and left side for observation--maximum arrow = 7.35 m/s........... 19

6. Comparison of surface data--thin lines for simulation and thick lines for observation, wind direction, and windspeed--temperatures at 2- and 10-m levels, dew point, and downward shortwave radiation as a function of time for station S1............................. 20

7. Comparison of surface data--thin lines for simulation and thick lines for observation, wind direction, and windspeed--temperatures at 2- and 10-m levels, dew point, and downward shortwave radiation as a function of time for station C1............................. 21

8. Vertical distributions of wind direction and windspeed, and horizontal components of wind vectors, temperature, and dew point--thin lines for simulation and thick lines for observation.............. 22

9. Vertical distributions of wind direction and windspeed, and horizontal components of wind vectors, temperature, and dew point--thin lines for simulation and thick lines for observation.............. 23

10a. Time series of wind direction and windspeed at 800-, 400-, and 200-m levels for station = 03................................ 24

10b. Time series of wind direction and windspeed at 100-, 50-, and 10-m levels for station = 03................................. 25

11a. Time series of temperature and dew point at 800-, 400-, and 200-m levels for station = 03................................ 26

11b. Time series of temperature and dew point at 100-, 50-, and 10-m levels for station = 03................................. 27

12. Time series of wind direction and windspeed at 500-, 700-, 850-mbar levels for station = 03................................. 28

13. Time series of temperature and dew point at 500-, 700-, and 850-mbar levels for station = 03............................. 29

14. Time series of statistical parameters for surface wind data......... 30

15. Time series of statistical parameters for surface (10-m level) temperature.. 31

16. Time series of average differences between observation and simulation for horizontal wind vector components, speed, temperature, dew point, and pressure at the 10-m level.......................... 32

17. Time series of average differences between observation and simulation for horizontal wind vector components, speed, temperature, dew point, and pressure at the 1000-m level........................ 33

18. Time series of correlation coefficients of horizontal wind vector components, speed, temperature, dew point, and pressure for the 10-m level... 34

19. Time series of correlation coefficients of horizontal wind vector components, speed, temperature, dew point, and pressure for the 1000-m level... 35

1. INTRODUCTION

In 1992, the U.S. Army will sponsor the workshop on mesoscale model technology exchange. The workshop will be handled by the MESOMET Panel. The objectives of the workshop are the following:*

- to identify state-of-the-art technology of mesoscale modeling;
- to inform the scientific community about the availability of Project WIND (wind in non-uniform domains) data; and
- to serve as a forum for mesoscale modeling technology exchange.

The U.S. Army Atmospheric Sciences Laboratory (ASL) will be assigned to examine the subset of the outputs that are generated by eight different mesoscale models.

In the last several months, several computer programs to examine and display the outputs of the mesoscale model to compare with observations, have been developed by ASL using the output of a mesoscale model HOTMAC (High Order Turbulence Model for Atmospheric Circulation) (Yamada and Bunker, 1989) and Project WIND Phase I, Julian days 178-179, data (Cionco, 1990). Programs developed consist of those displaying horizontal, vertical, and temporal distributions of meteorological parameters--simulated and observed.

This report describes the methods used to examine model output and show examples of graphic display. Detailed results of comparisons between model simulation and observation will be described in the near future. The computer programs are developed by using the FORTRAN language with the National Center for Atmospheric Research (NCAR) GKS-Compatible Graphic System. The programs are on the HP 9000/840 computer at ASL.

2. PROJECT WIND DATA AND MODEL SIMULATION

Data used to develop the program was from Project WIND Phase I, covering 24 h from 0900 l.s.t. of day 178. These measurements consisted of upper-air sounding data at five locations every 2 h, with a few missing data, and 21 surface station data. Details of the data set are presented in Cionco (1990).

Model simulation was conducted over terrain as shown in figure 1.** Latitude and longitude of the southwestern corner of the domain are 39° 11' 04.4" N and 122° 59' 58" W. The terrain heights were represented by grids of 81 by 81 with a unit grid distance of 2.5 km. The highest and lowest grid points are 2477 and 12 m, respectively, above sea level. In the figure, numbers represent the locations of upper-air stations. Meteorological parameters were calculated at every other grid point (40 by 40) for 16 vertical layers, using HOTMAC. The model was initialized at 0900 l.s.t. of day 178 using sounding data taken at station 04, and simulation continued until 0800 l.s.t. of the next day.

---

*J. E. Harris and R. E. Meyers, 1991, Trip report on meeting of MESOVET Panel in Bruges, Belgium, 9-10 May 1991 (unpublished).

**Figures are presented at the end of the text.

In figure 1b the locations of surface observations are marked. Surface data contained windspeed, wind direction, temperature, relative humidity, pressure, incoming solar radiation, and precipitation. During the 24-h period (between 0900 l.s.t. of day 178 and 0900 l.s.t. of day 179), no precipitation occurred. Therefore, precipitation data was not examined. Relative humidity data was converted to dew point by using empirical formulas.

3. DATA INTERPOLATION METHODS

3.1 Upper-Air Data

Generally, most mesoscale models are formulated on terrain-following coordinates, and meteorological parameters are calculated at particular heights determined by model design. To compare model output with observation at a desired height, one must interpolate both model outputs and observed data to the height. Model output values computed at a grid point most adjacent to an upper-air sounding station were used for the comparison study.

In HOTMAC model, the following equation is used to define a terrain-following vertical coordinate.

$$z^* = \overline{H}\frac{z - z_g}{H - z_g} \tag{1}$$

where z^* and z are the transformed and Cartesian vertical coordinates, respectively; z_g is ground elevation above sea level; $\overline{H}$ is the material surface top of the model; and H is the corresponding height in the coordinate. For simplicity, H is specified as

$$H = \overline{H} + z_{gmax} \tag{2}$$

where z_{gmax} is the maximum value of z_g. From equation (1), height above ground H_g can be given as

$$H_g = z - z_g = z^* \frac{\overline{H} + z_{gmax} - z_g}{\overline{H}} \tag{3}$$

The author applied both linear interpolation and cubic spline methods to interpolate the values of meteorological parameters (horizontal wind components, temperature, and dew point) at desired height above ground. Few differences were found in the results produced by the two methods. In the linear interpolation method, meteorological parameter φ at height z can be obtained by using the values at z_i and z_{i+1}, where $z_i < z < z_{i+1}$, as follows: (figure 2)

$$\varphi(z) = A \cdot \varphi_i + B \cdot \varphi_{i+1} \tag{4}$$

where

$$A = \frac{z_{i+1} - z}{z_{i+1} - z_i} \tag{5}$$

$$B = \frac{z - z_i}{z_{i+1} - z_i} \quad . \tag{6}$$

The equation for cubic spline interpolation is expressed as

$$\varphi(z) = A \cdot \varphi_i + B \cdot \varphi_{i+1} + C \cdot \varphi''_i + D \cdot \varphi''_{i+1} \tag{7}$$

where

$$C = \frac{1}{6} \cdot (A^3 - A) \cdot (z_{i+1} - z_i)^2 \tag{8}$$

$$D = \frac{1}{6} \cdot (B^3 - B) \cdot (z_{i+1} - z_i)^2 \tag{9}$$

and

$$\varphi'' = \frac{d^2\varphi}{dz^2} \quad . \tag{10}$$

FORTRAN programs of cubic spline interpolation described in Press et al. (1989) were used.

3.2 Surface Data

To reduce the value of a meteorological parameter at a surface station k, values at four grid points surrounding the station were used as

$$\varphi_k = \frac{\sum_i \varphi_i \frac{1}{r_i^2}}{\sum_i \frac{1}{r_i^2}} \quad , \tag{11}$$

where the subscript i represents a grid point, r_i is the distance between station location and grid point i, and φ is an arbitrary meteorological parameter.

4. SURFACE METEOROLOGICAL PARAMETERS

4.1 Horizontal Distributions of Gridded Data

Plotting horizontal distributions of gridded data of model output is important to examine distribution patterns of meteorological parameters over the model domain and to intercompare between models. Scalar variables such as temperature and sensible heat flux are plotted by using contour-line drawing routines in the NCAR GKS-Compatible Graphic System. Horizontal wind vectors are plotted by using vector drawing routines. In the following figures, (a) and (b) represent daytime and nighttime conditions for 1500 l.s.t. of day 178 and 0300 l.s.t. of day 179, respectively.

Examples of contour-line plotting of scalar variables are shown in figures 3 and 4. Figures 3a and 3b show air temperature distributions at 10-m levels above ground. Contour lines are drawn with 5 °C intervals. Terrain contour lines are also drawn using thin lines. Figure 4 shows the distribution of sensible heat flux (W/m^2). Sensible heat fluxes are upward (positive) throughout the model domain during the day, and downward (negative) during the night. Upward fluxes are contoured by solid lines and downward fluxes by broken lines.

Figure 1b shows that surface observation stations were in the center of the model domain. For easier comparison, the right side of figures 5a and 5b show the horizontal wind vectors computed by the model for the center area only; the left side shows the observed wind vectors. Upslope wind conditions during the day and downslope wind conditions during the night were well simulated and in good agreement with observations.

4.2 Comparisons of Simulation with Surface Observation

The computer program developed for comparing simulation with surface observation takes the following steps:

- determines the locations of surface station in grid coordinate.
- creates time series arrays of meteorological parameters for points representing surface stations, using data at four grid points surrounding the surface stations.

The program is designed to plot both simulation and observation for any surface station desired.

Since the model output file contained hourly data at grid points, time series plotting of both simulated and observed data were also made hourly. Wind direction and windspeed (meters per second), temperatures (degrees Celsius) at 2- and 10-m levels, dew point (degrees Celsius), and downward shortwave radiation (watts per square meter) were plotted. As examples, plottings for stations S1 and C1 are shown, respectively, in figures 6 and 7, with thin lines representing simulation and thick lines representing observation. These figures show that shortwave radiation observation data and temperatures at either level were not available at some stations.

5. UPPER-AIR METEOROLOGICAL PARAMETERS

5.1 Vertical Distributions at the Locations of Sounding Stations

Upper-air data were observed at five stations during the 24-h period. Data were taken at each station every 2 h, with some exceptions. The program developed to plot vertical distributions of meteorological parameters extracts data at grid points closest to the stations and creates arrays of data for each station. The program was arranged so plotting could be made for a desired station and time.

Figure 8 shows the vertical distributions of wind direction and windspeed, x and y components of wind vector, temperature, and dew point for station 01 and 1300 l.s.t. of day 178. Thin and thick lines represent, respectively, simulation and observation. Figure 9 shows station 04 at 0100 of day 179.

5.2 Time-Series at Different Levels

For comparison between different models, it is convenient to have meteorological parameters at the same heights. Participants in the workshop of mesoscale model technology e ̲hange are asked to produce time series of meteorological parameters at the following: standard heights 2, 10, 50, 100, 200, 400, 800 m above the ground and standard pressure levels of 850, 700, 500, and 300 mbar. The HOTMAC model computed variables at the following 16 levels of terrain-following coordinates: 0, 2, 6, 10, 14, 28, 114, 281, 530, 861, 1273, 1767, 2342, 3000, 3729, 4559. Thus, interpolation of variables from model height to standard height was necessary. As described in section 3, a cubic spline interpolation method was used for interpolation from model heights to standard heights. The linear interpolation method was used to interpolate to standard pressure level. In the HOTMAC model, pressure is a diagnostic variable.

The program extracts parameters for grid points most adjacent to upper-air stations and calculates the values at standard heights or pressure levels. Observed data were also interpolated by using cubic spline or linear interpolation methods. Time series arrays of meteorological parameters for different station locations and standard levels were generated; therefore, time series of plotting could be easily made for different stations and levels. Wind direction and windspeed, temperature, and dew point were plotted.

Figures 10a and 10b show the time series of wind direction and windspeed at seven different heights for station 03. Continuous lines are used for simulation and asterisks (*) are used to plot the values of observation. Figures 11a and 11b show examples of the time series of temperature and dew point.

Time series for three different pressure levels (500, 700, and 850 mbar) are given in figures 12 and 13. Neither observation nor simulation was available at the 300-mbar level. Plots for station 03 were used for these figures.

6. EVALUATION OF MODEL PERFORMANCE

Visual comparisons of simulation with observations (as shown in the previous sections) are useful. However, model performance evaluated quantitatively is also desirable since it enables us to compare objectively one model to another model and to gain insight into the sources of error. For the present simulation, continuous data of wind direction, windspeed, temperature, and humidity were available throughout the 24-h period at 21 surface stations; and 4 or 5 upper-air sounding data were available every 2 h. These data were used to perform the following statistical evaluations.

6.1 Surface Data

Mean, standard deviation, root mean square errors (rmse), unbiased rmse, and agreement measure were calculated hourly. Willmott (1981, 1982) and Willmott et al. (1985) recommend the use of the above statistical parameters to quantitatively evaluate model performance. The following equations are definitions of these parameters:

a. mean

$$\overline{\varphi} = \frac{\sum_k \varphi(k)}{N} \tag{12}$$

where $\varphi(k)$ is meteorological parameters at kth station, and N is the number of stations. Means for both simulation and observation were calculated. In a good agreement case, means for both should have similar values.

b. rmse (E) and unbiased rmse (E_{ub})

$$E = \left\{ \frac{\sum_k [\varphi_m(k) - \varphi_o(k)]^2}{N} \right\}^{1/2} \tag{13}$$

$$E_{ub} = \left\{ \sum_k \frac{[(\varphi_m(k) - \overline{\varphi_m}) - (\varphi_o(k) - \overline{\varphi_o})]^2}{N} \right\}^{1/2} \tag{14}$$

If there is a perfect agreement, E and E_{ub} are zero.

c. standard deviation

$$\sigma = \left\{ \sum_k \frac{[\varphi(k) - \overline{\varphi}]^2}{N} \right\}^{1/2} \tag{15}$$

In a good agreement case, the standard deviation for both simulation and observation should have similar values.

d. agreement measure

$$A = 1 - \frac{\sum_k (\varphi_m(k) - \varphi_o(k))^2}{\sum_k (|\varphi_m(k) - \overline{\varphi_o}| + |\varphi_o(k) - \overline{\varphi_o}|)^2} \;. \tag{16}$$

This dimensionless index has a theoretical range of 1.0 (for perfect agreement) to 0.0 (for no agreement).

These statistical parameters were calculated hourly for wind, temperature, and dew point. Figure 14 shows the results for wind. Mean wind direction was calculated from the means of horizontal wind components. Thin lines represent simulation and thick lines represent observation in the top three portions of figure 14. In the rmse plotting, E_b was drawn using a thin line and E_{ub} by using a thick line. Agreement measure of windspeed was slightly lower during the daytime than during the night, as mean windspeed showed greater discrepancies during the day than during the night.

Figure 15 is a similar figure for temperature at the 10-m level. There is a good agreement between simulation and observation during the day, as can be seen in mean temperature and agreement measure. Agreement becomes poor during the night, as the standard deviation of observed temperature is much greater than that of simulation during the night, probably resulting from the model's incapability of representing localized effects. The rmse shows also that agreement between simulation and observation becomes poor during the night.

6.2 Upper-Air Data

So far, for upper-air data, the following two statistical parameters were calculated at different levels as a function of time to evaluate model performance. Different statistical parameters may need further consideration.

a. average difference between observation and simulation

$$\overline{\delta\varphi(t)} = \frac{\sum_k |\varphi_{k,o}(t) - \varphi_{k,m}(t)|}{N} \qquad (17)$$

where φ represents meteorological parameters, subscripts o and m are for observation and simulation, and N is the number of observations. $\delta\varphi$ of horizontal wind components, speed, temperature, dew point, and pressure were calculated at different levels every 2 h when observation of upper-air was available. Figures 16 and 17 are for the 10- and 1000-m levels, respectively. At the 10-m level, the difference of temperature becomes greater during the night, as has been mentioned in section 6.1. On the other hand, temperature difference at the 1000-m level did not show great difference at night, probably because temperature at the 1000-m level was influenced very little by surface heating and cooling. The average difference of the x component of wind at the 1000-m level grew after several hours of simulation. In this simulation, the model was initialized at 0900 l.s.t. using upper-air sounding data, and no adjustment was made during simulation.

b. correlation coefficient of variance

$$r(t) = \frac{\sum_k (\delta\varphi'_{k,o} \cdot \delta\varphi'_{k,m})}{\left(\sum_k \delta\varphi_{k,o}{}^2\right)^{1/2} \cdot \left(\sum_k \delta\varphi_{k,m}{}^2\right)^{1/2}} \tag{18}$$

where

$$\delta\varphi_o(t + \Delta t) = \varphi_o(t + \Delta t) - \varphi_o(t) \tag{19}$$

$$\delta\varphi_m(t + \Delta t) = \varphi_m(t + \Delta t) - \varphi_m(t) \tag{20}$$

$$\delta\varphi_o' = \delta\varphi_o - \overline{\delta\varphi_o} \tag{21}$$

$$\delta\varphi_m' = \delta\varphi_m - \overline{\delta\varphi_m} \tag{22}$$

Here the overline denotes an average of an entire simulation period. The use of the correlation coefficient of variance was suggested by the MESOMET panel.

The coefficient r(t) was calculated for meteorological parameters including horizontal wind components, windspeed, temperature, dew point, and pressure at different levels. Figures 18 and 19 show the 10- and 1000-m levels, respectively. The values of r(t) vary considerably for all the meteorological parameters. Ideas on model performance are difficult to obtain from these figures. The correlation coefficient must be done carefully.

7. CONCLUDING REMARKS

This report describes and illustrates computer programs developed for a comparison between model simulation and observation by using Project WIND Phase I day 178 data and the HOTMAC model output. Temporal and spatial comparisons of simulation with observation can be made by using the program developed. Statistical parameters described in the report will become meaningful when different model simulations are compared with observations.

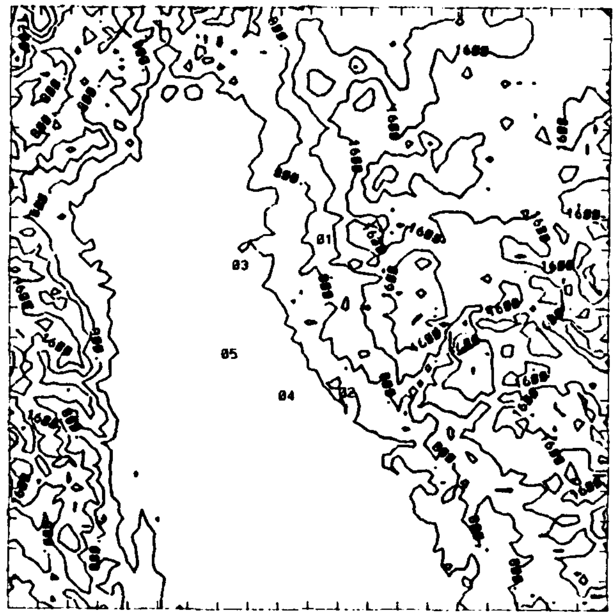

(a) Locations of upper-air sounding stations, marked with numerical numbers.

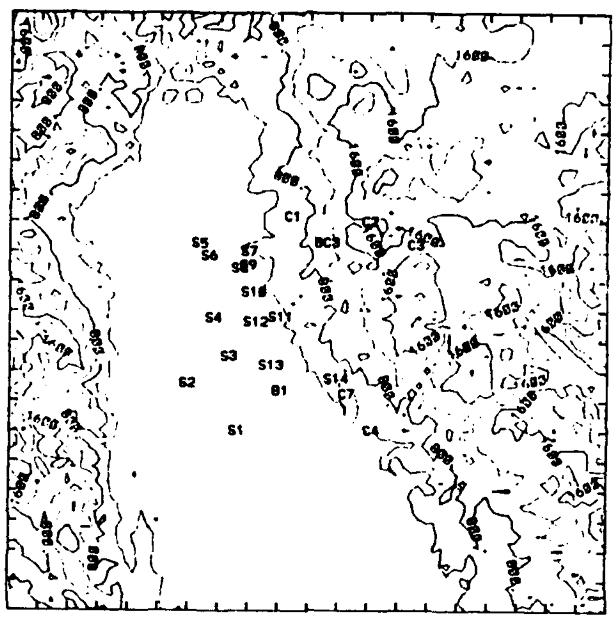

(b) Locations of surface stations.

Figure 1. Project WIND terrain map, with 400 m height contours.

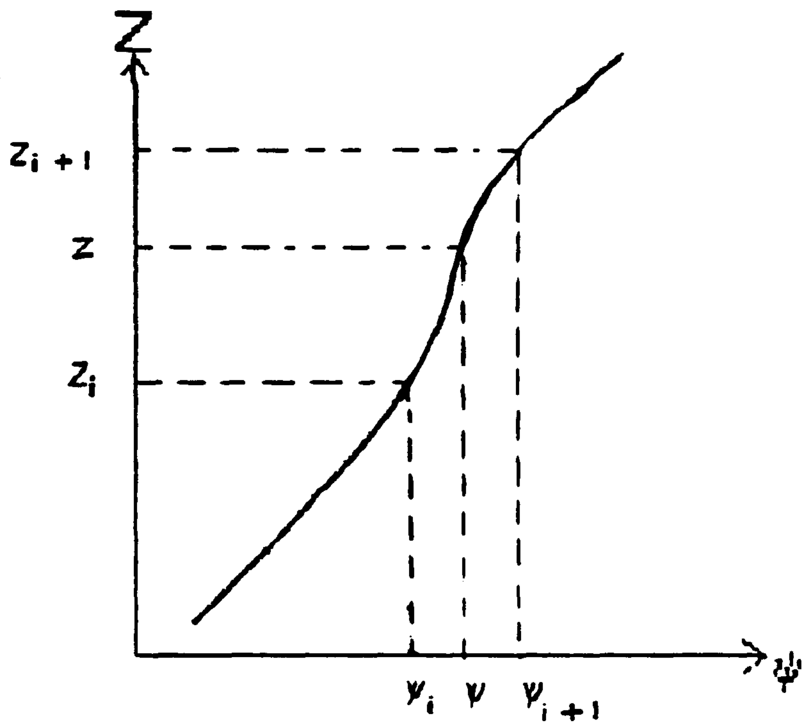

Figure 2. Interpolation method of vertical data.

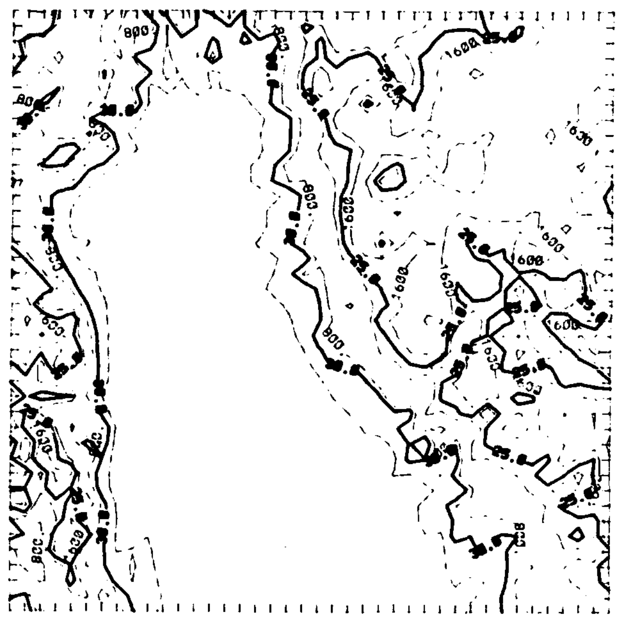

(a) 1500 l.s.t., day 178

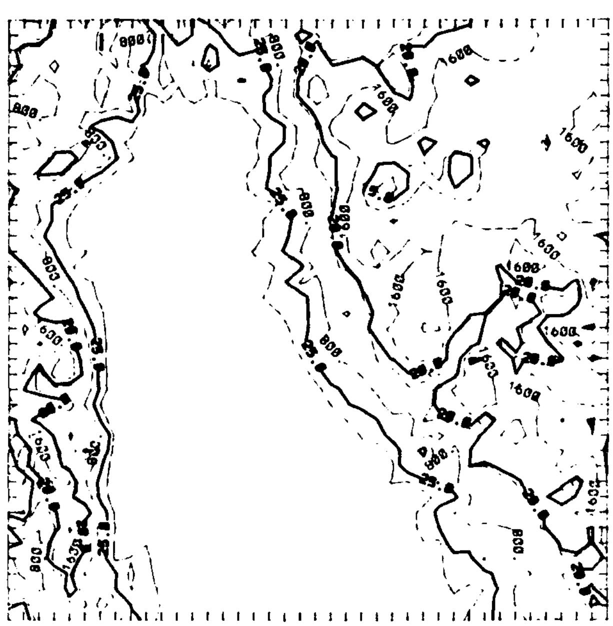

(b) 0300 l.s.t., day 179

Figure 3. Temperature distribution with 5 °C contours.

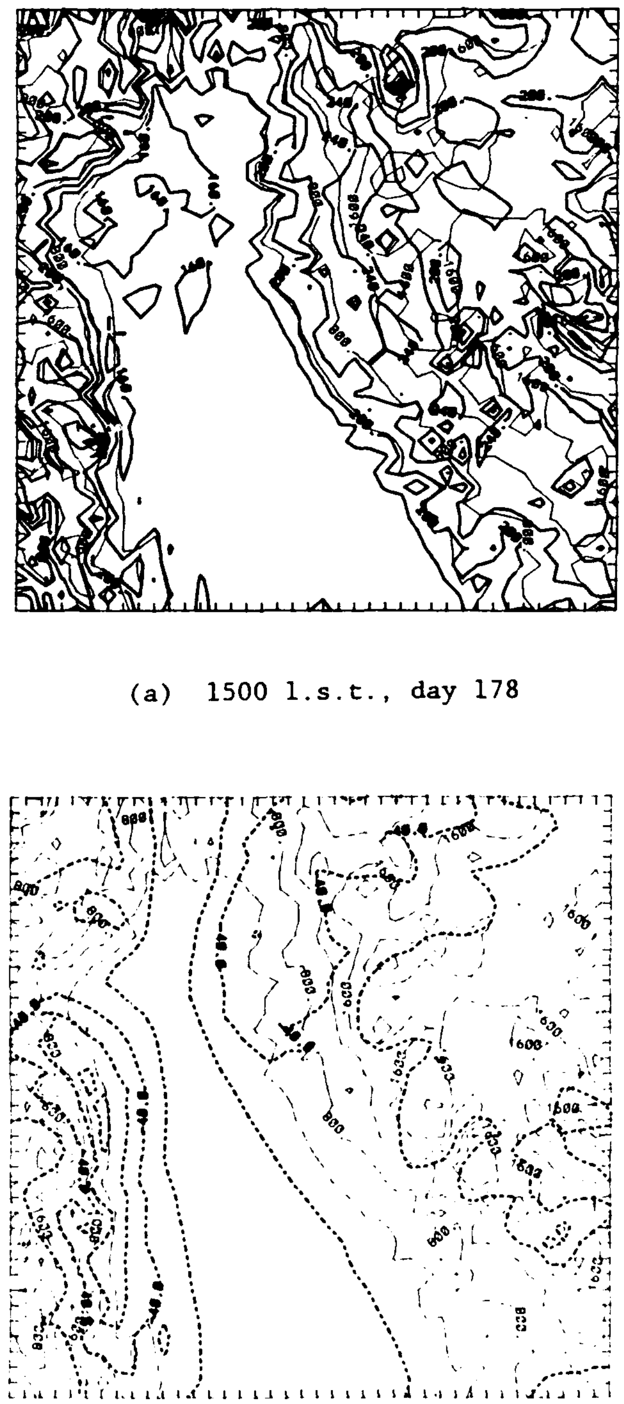

(a) 1500 l.s.t., day 178

(b) 0300 l.s.t., day 179

Figure 4. Sensible heat flux distribution over terrain data--solid lines for upward flux and broken lines for downward flux.

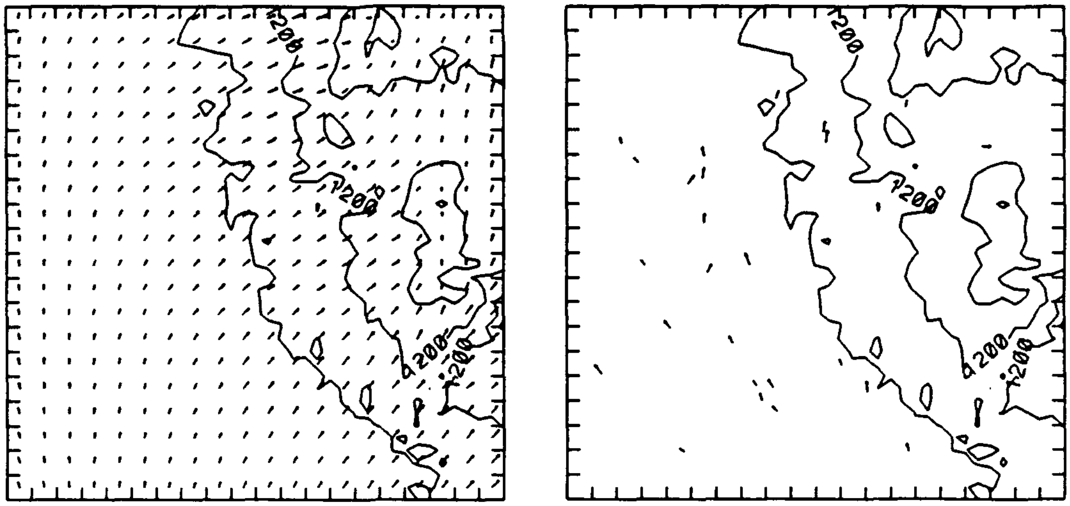

(a) 1500 l.s.t., day 178

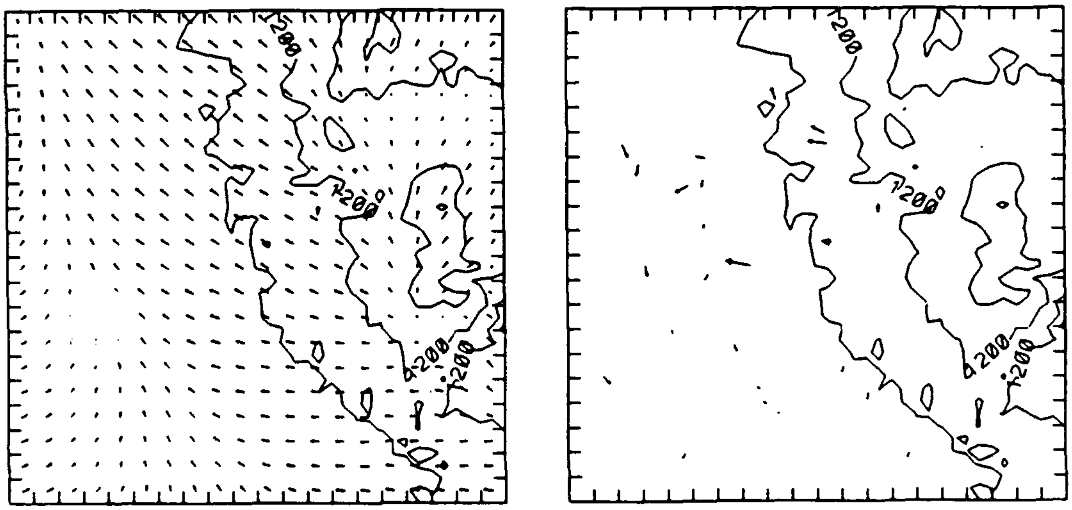

(b) 0300 l.s.t., day 179

Figure 5. Horizontal wind vector distributions--right side for simulation and left side for observation--maximum arrow = 7.35 m/s.

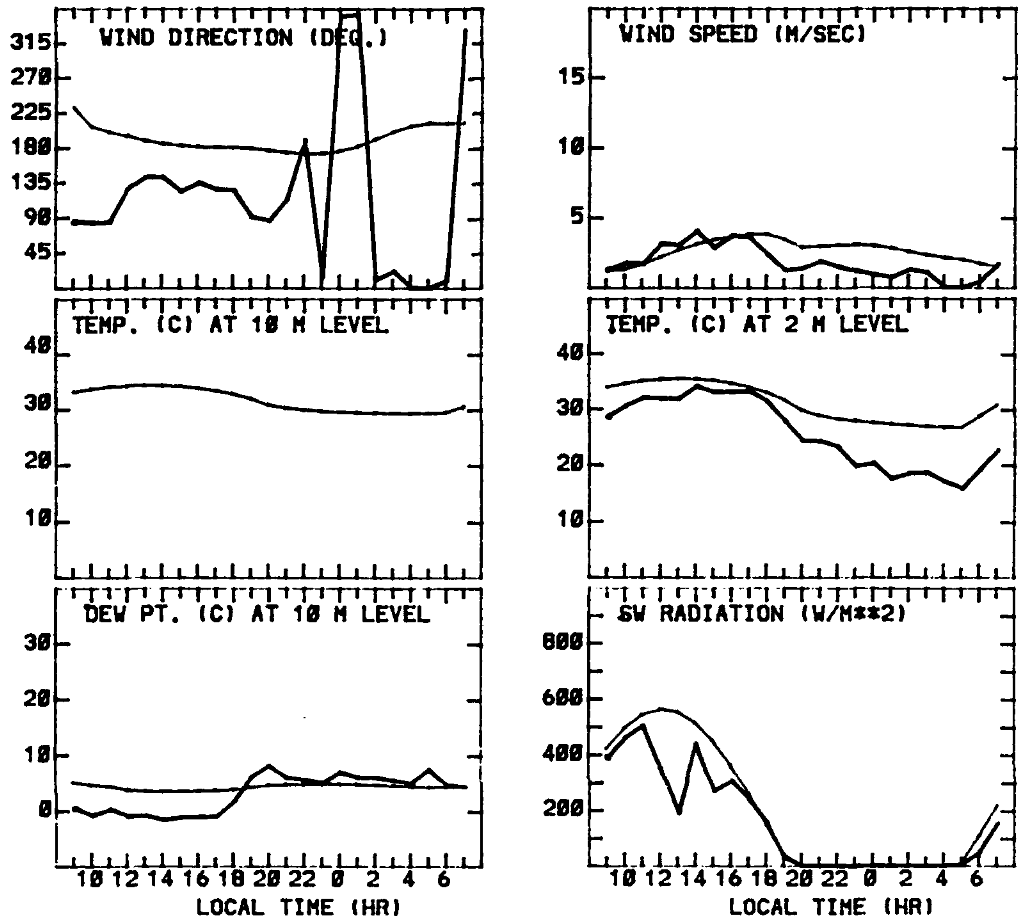

Figure 6. Comparison of surface data--thin lines for simulation and thick lines for observation, wind direction, and windspeed--temperatures at 2- and 10-m levels, dew point, and downward shortwave radiation as a function of time for station S1.

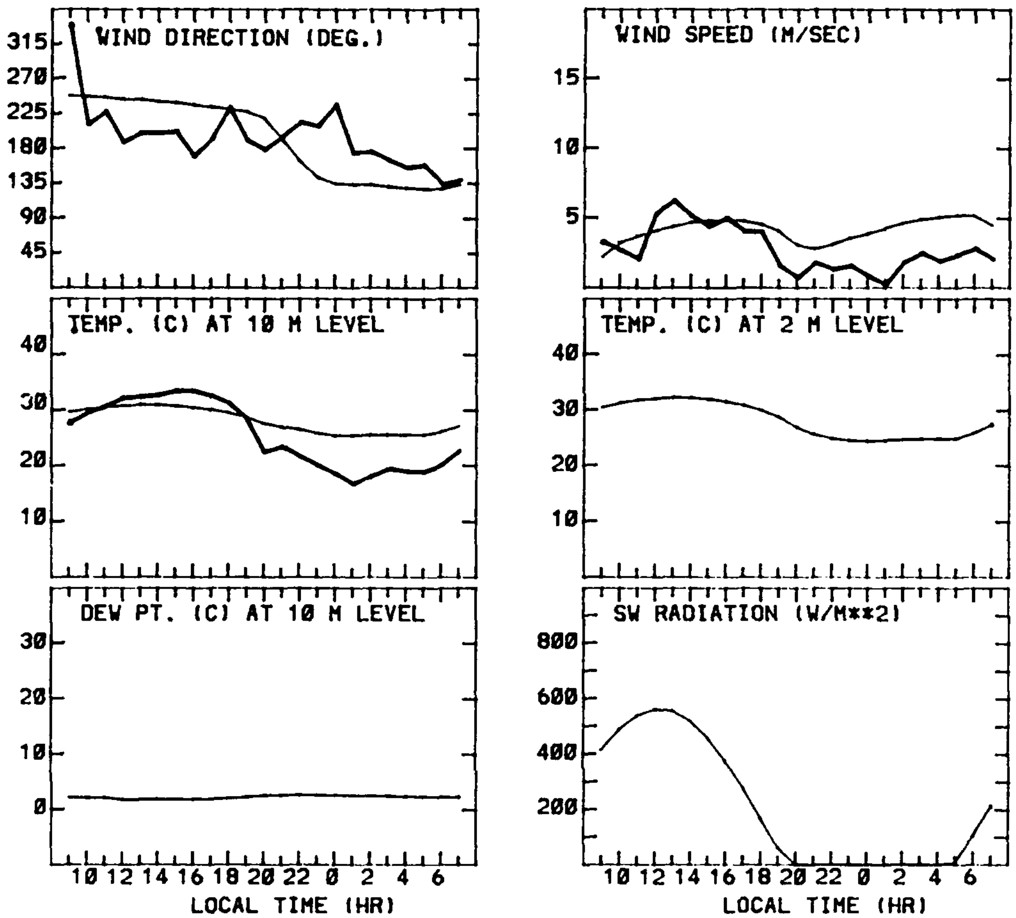

Figure 7. Comparison of surface data--thin lines for simulation and thick lines for observation, wind direction, and windspeed--temperatures at 2- and 10-m levels, dew point, and downward shortwave radiation as a function of time for station C1.

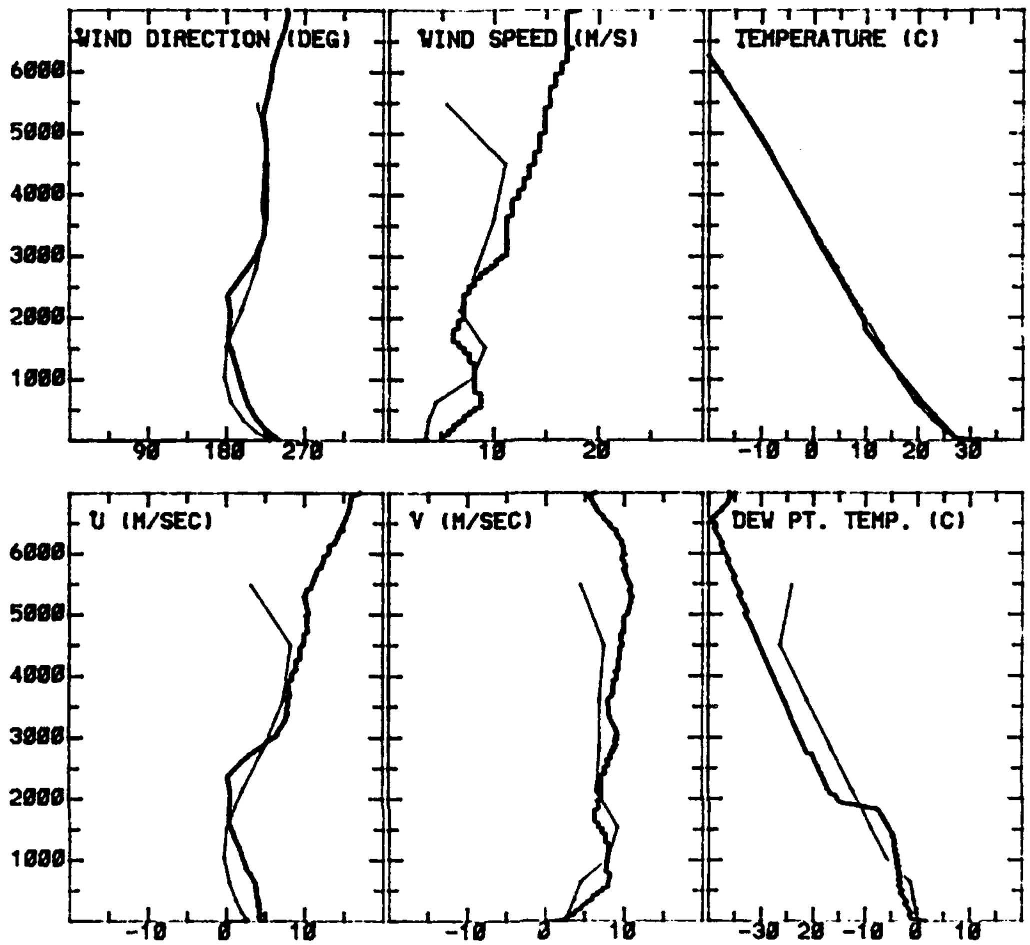

Figure 8. Vertical distributions of wind direction and windspeed, and horizontal components of wind vectors, temperature, and dew point--thin lines for simulation and thick lines for observation. Station = 0.1, 1300 l.s.t., day 178.

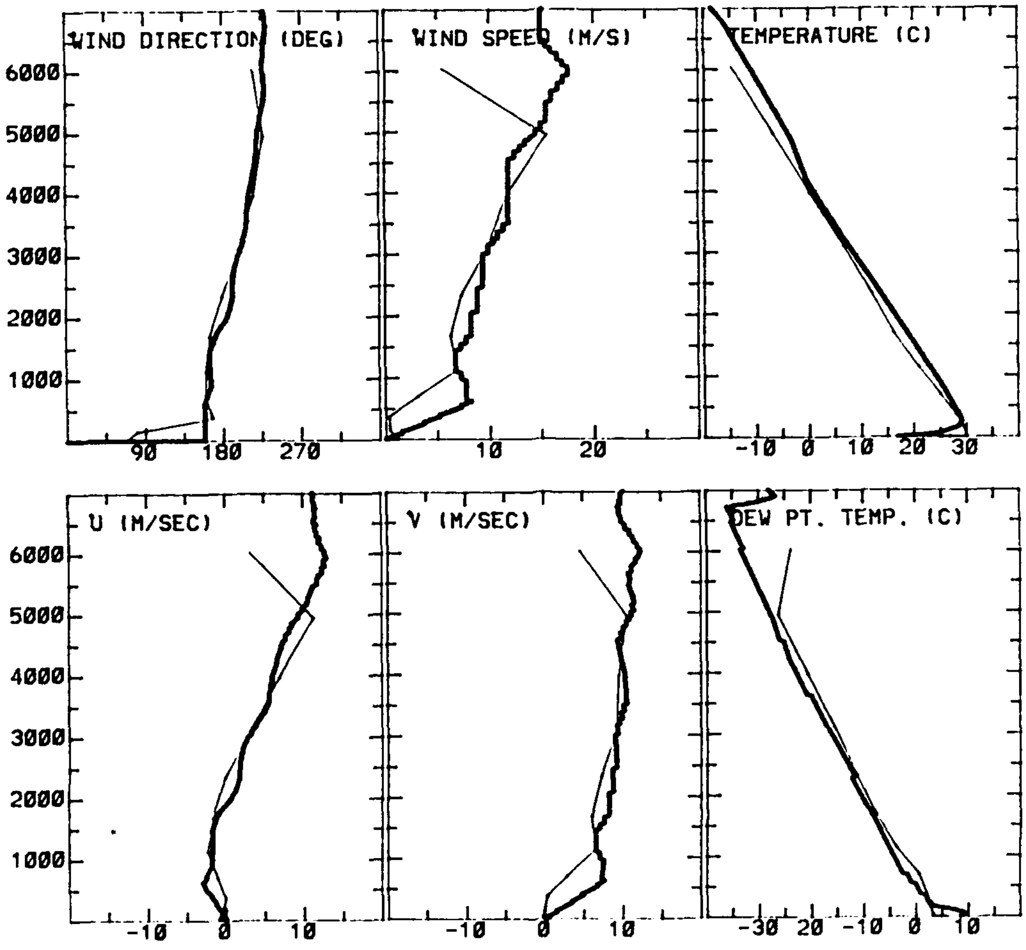

Figure 9. Vertical distributions of wind direction and windspeed, and horizontal components of wind vectors, temperature, and dew point--thin lines for simulation and thick lines for observation. Station = 04, 0100 l.s.t., day 179.

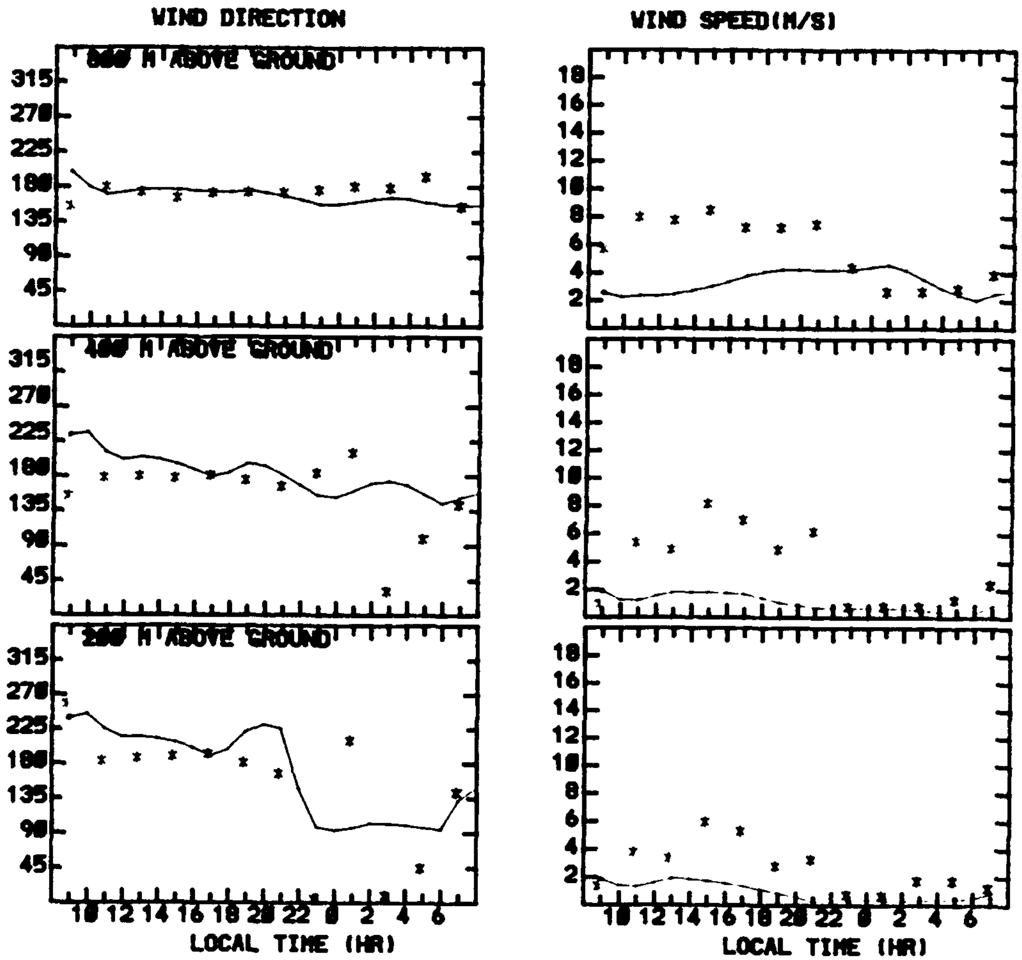

Figure 10a. Time series of wind direction and windspeed at 800-, 400-, and 200-m levels for station = 03.

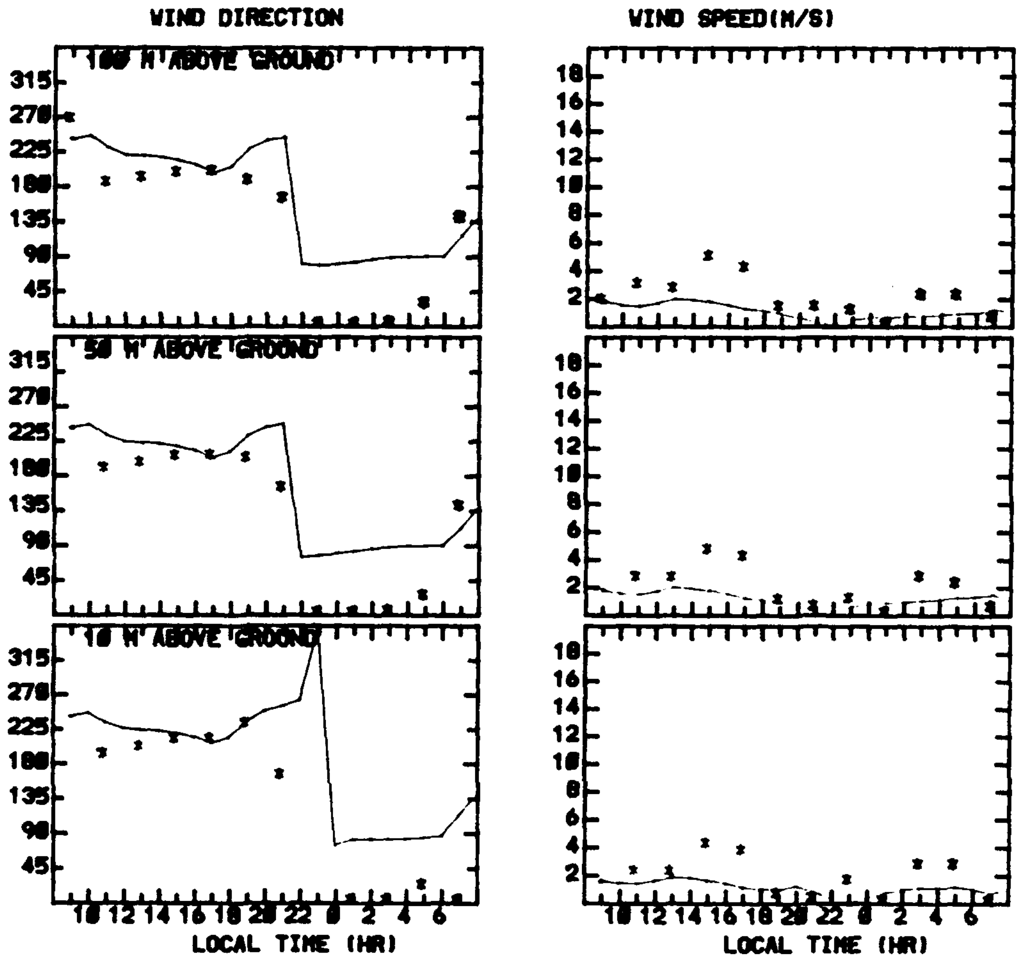

Figure 10b. Time series of wind direction and windspeed at 100-, 50-, and 10-m levels for station = 03.

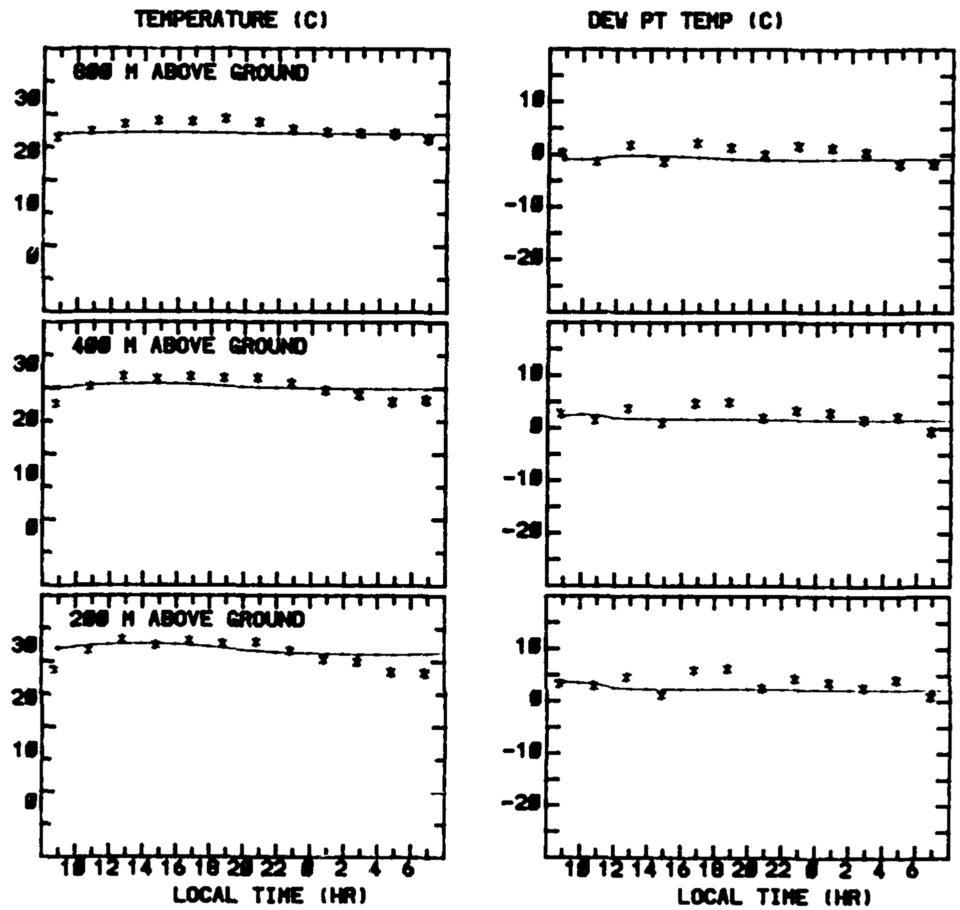

Figure 11a. Time series of temperature and dew point at 800-, 400-, and 200-m levels for station = 03.

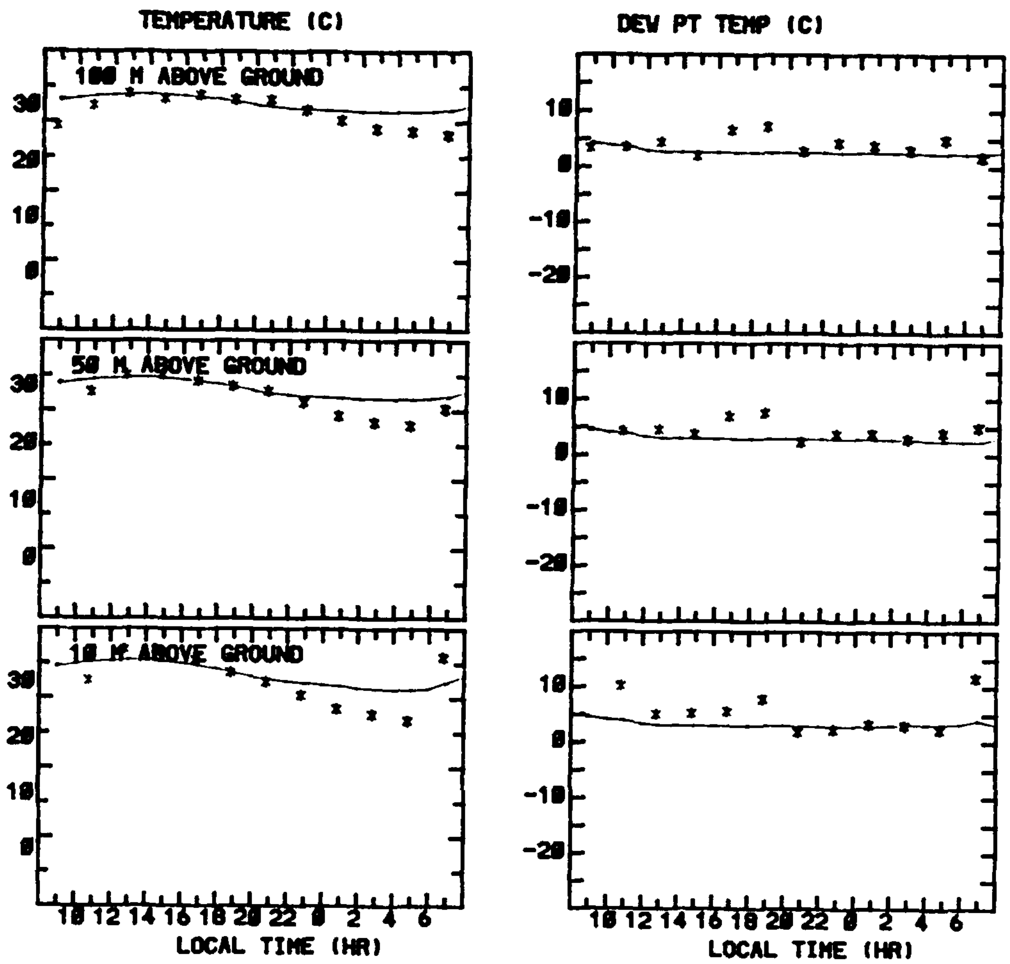

Figure 11b. Time series of temperature and dew point at 100-, 50-, and 10-m levels for station = 03.

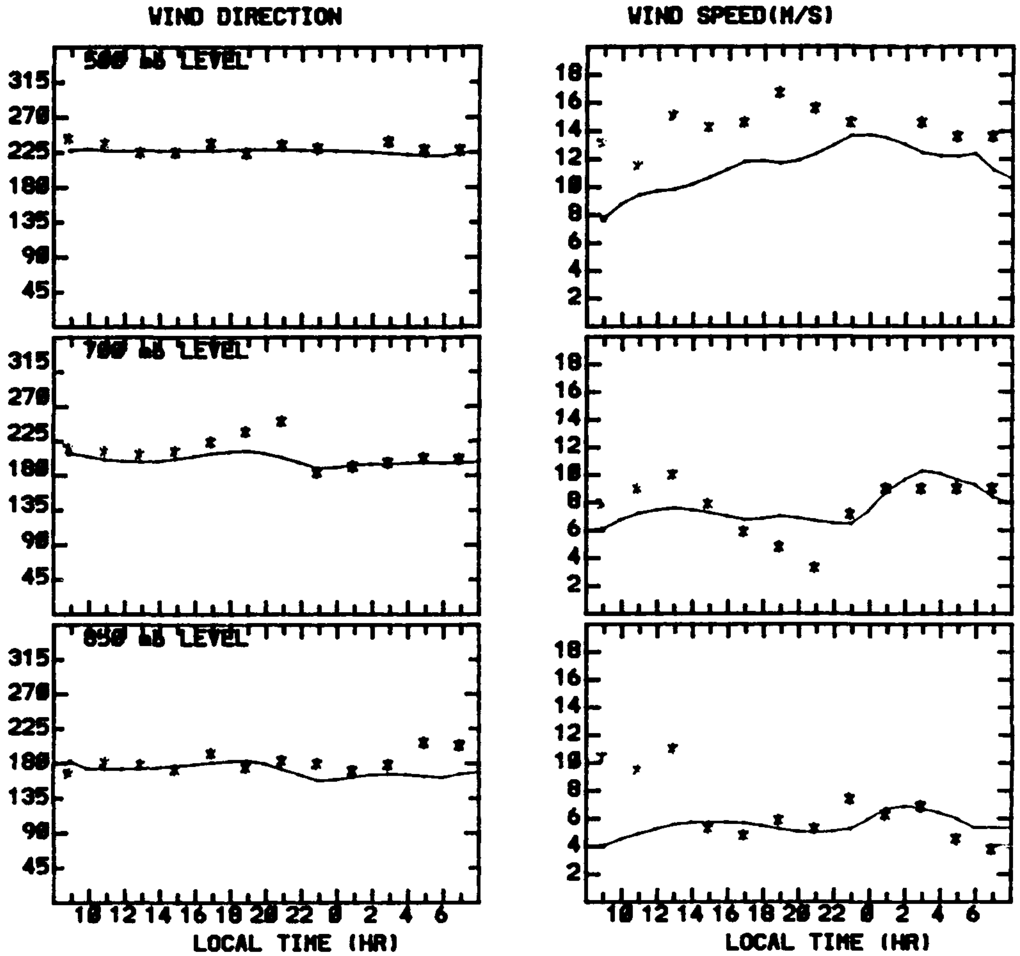

Figure 12. Time series of wind direction and windspeed at 500-, 700-, and 850-mbar levels for station = 03.

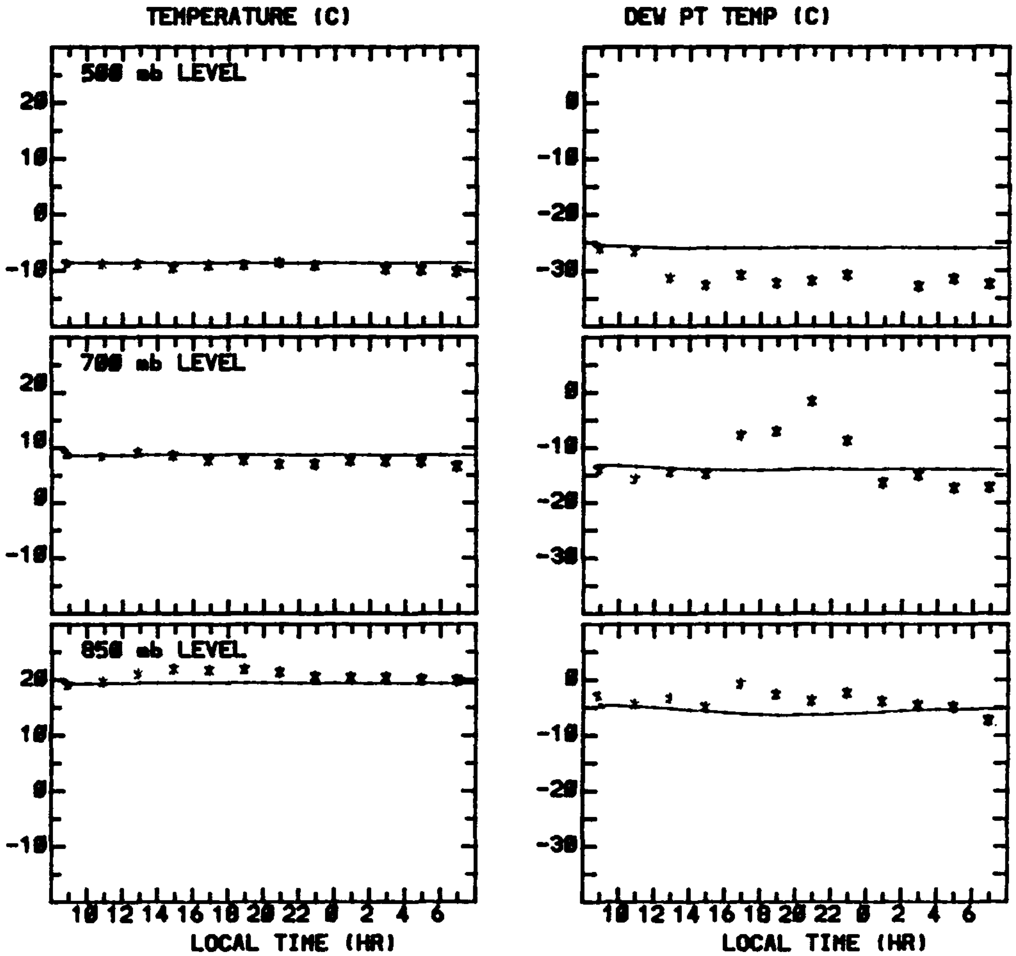

Figure 13. Time series of temperature and dew point at 500-, 700-, and 850-mbar levels for station = 03.

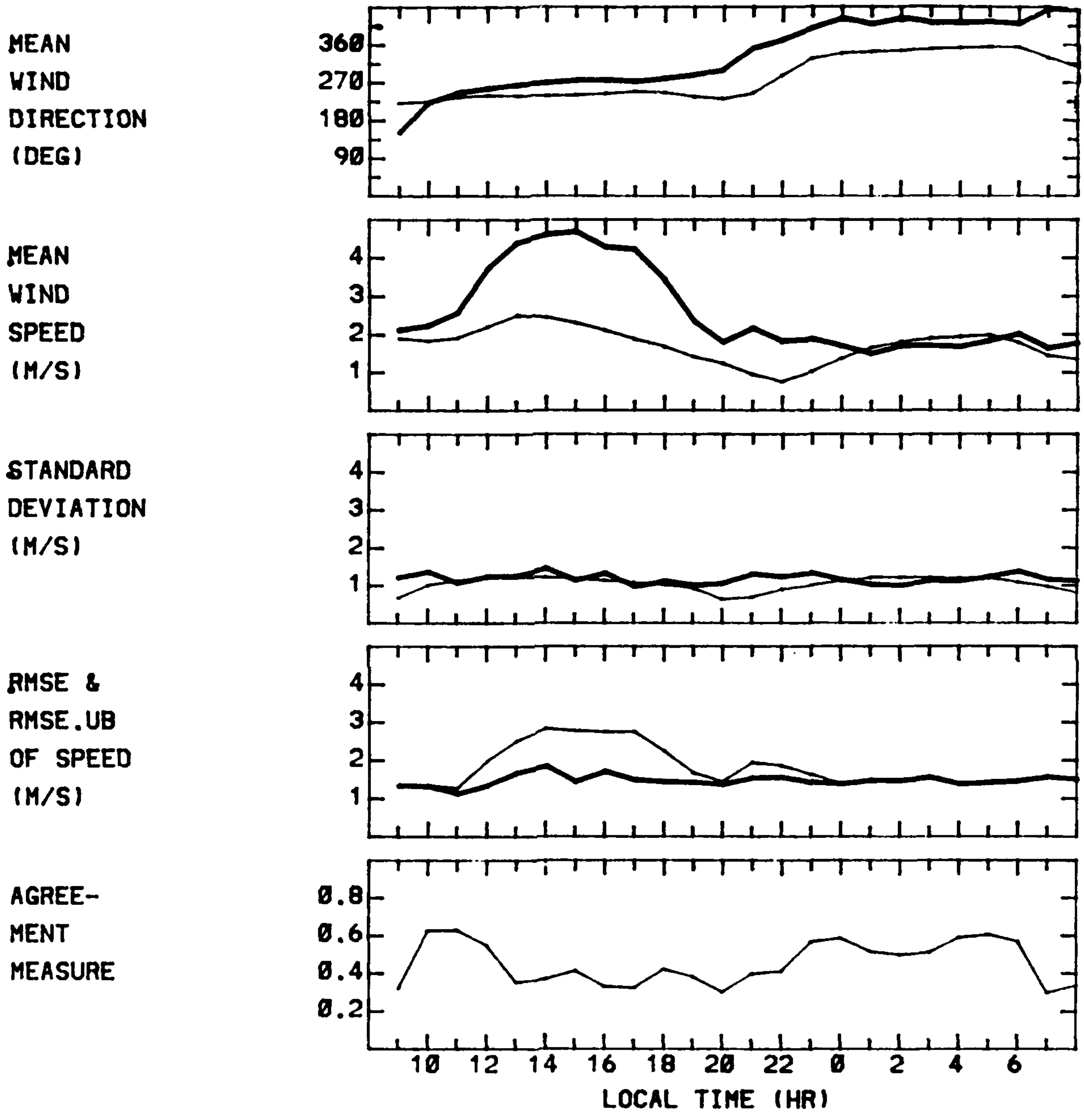

Figure 14. Time series of statistical parameters for surface wind data. Mean wind direction and windspeed, standard deviation, rmse, and agreement measure. In the top three portions of the figure, the thin lines are for simulation and the thick lines are for observation. In the fourth portion (rmse), the thin line is for E_b and the thick is for E_{ub}.

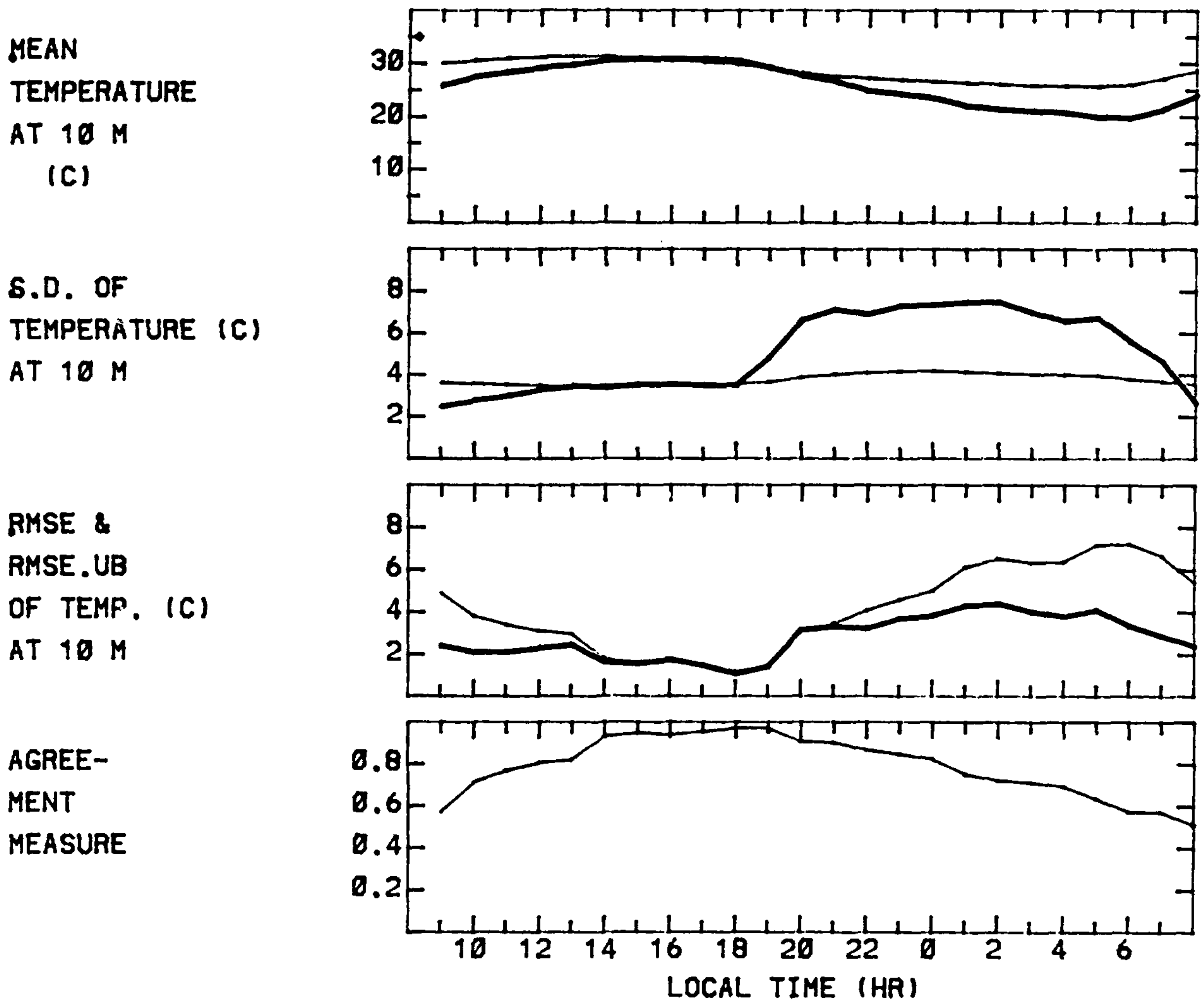

Figure 15. Time series of statistical parameters for surface (10-m level) temperature. In the top two portions of the figure, the thin lines are for simulation and the thick lines are for observation. In the third portion, the thin line is for E_b and the thick line is for E_{ub}.

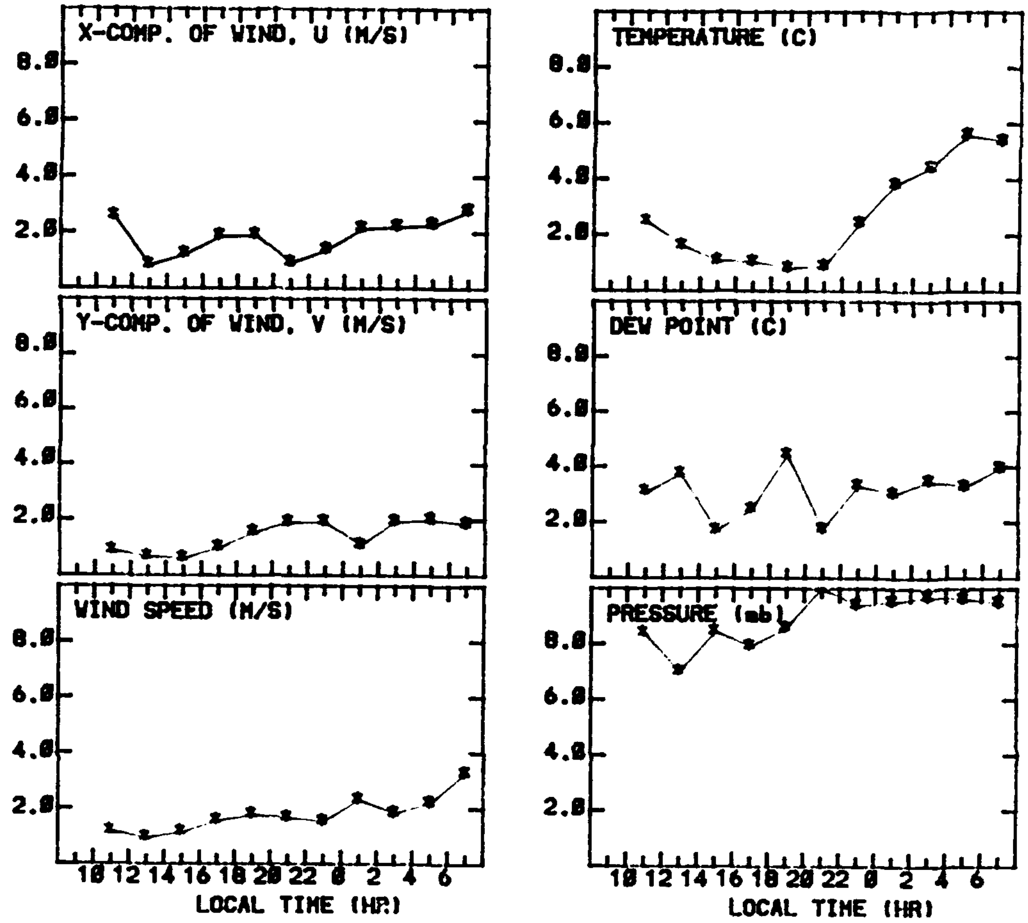

Figure 16. Time series of average differences between observation and simulation for horizontal wind vector components, speed, temperature, dew point, and pressure at the 10-m level.

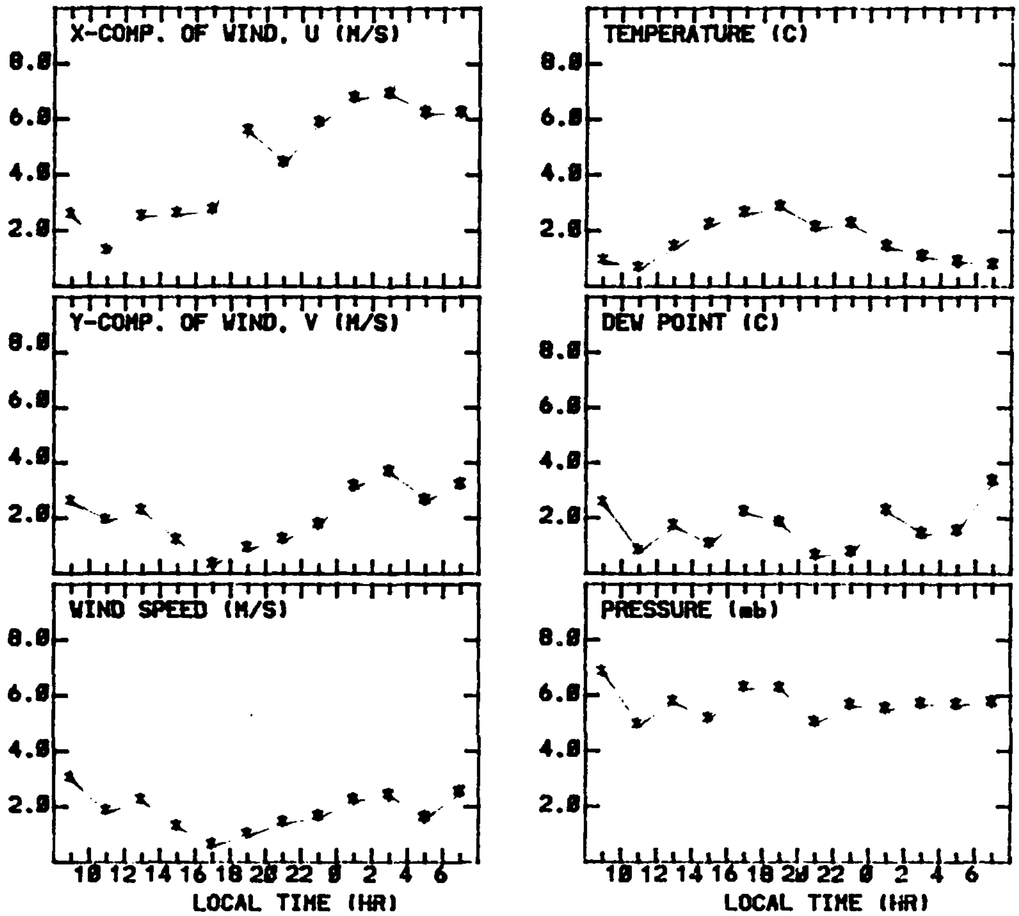

Figure 17. Time series of average differences between observation and simulation for horizontal wind vector components, speed, temperature, dew point, and pressure at the 1000-m level.

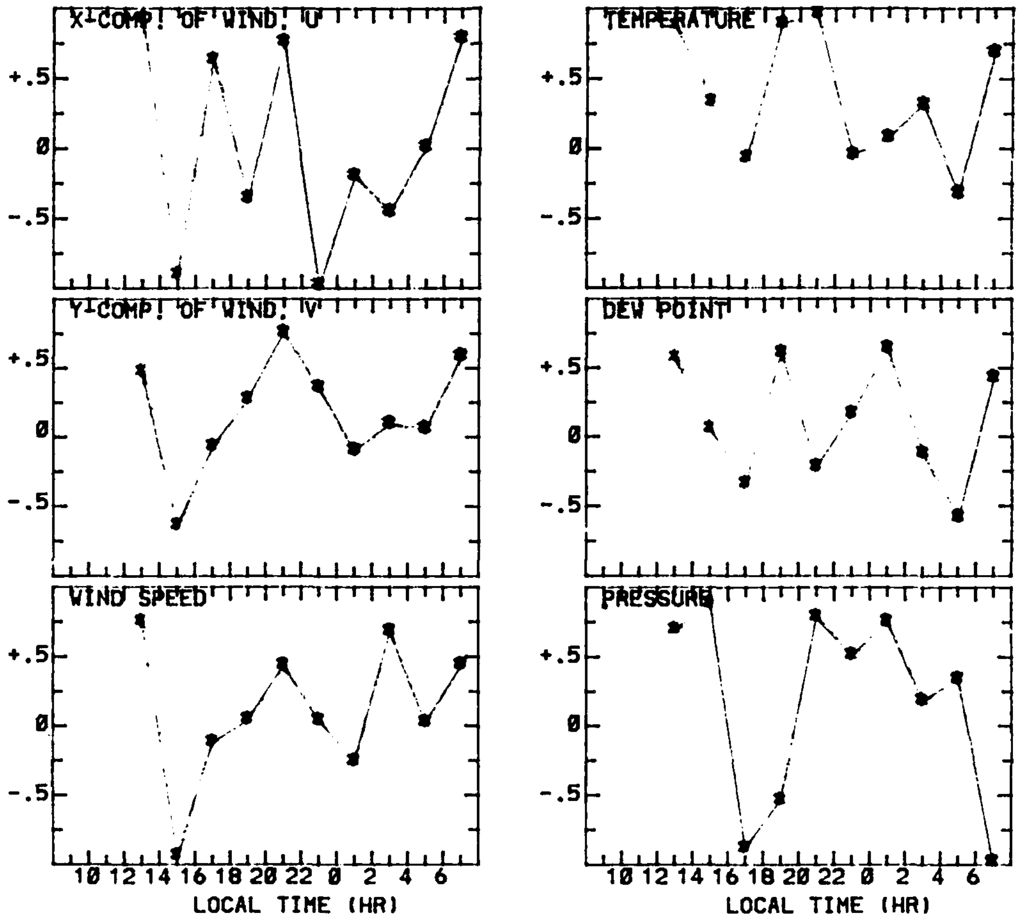

Figure 18. Time series of correlation coefficients of horizontal wind vector components, speed, temperature, dew point, and pressure for the 10-m level.

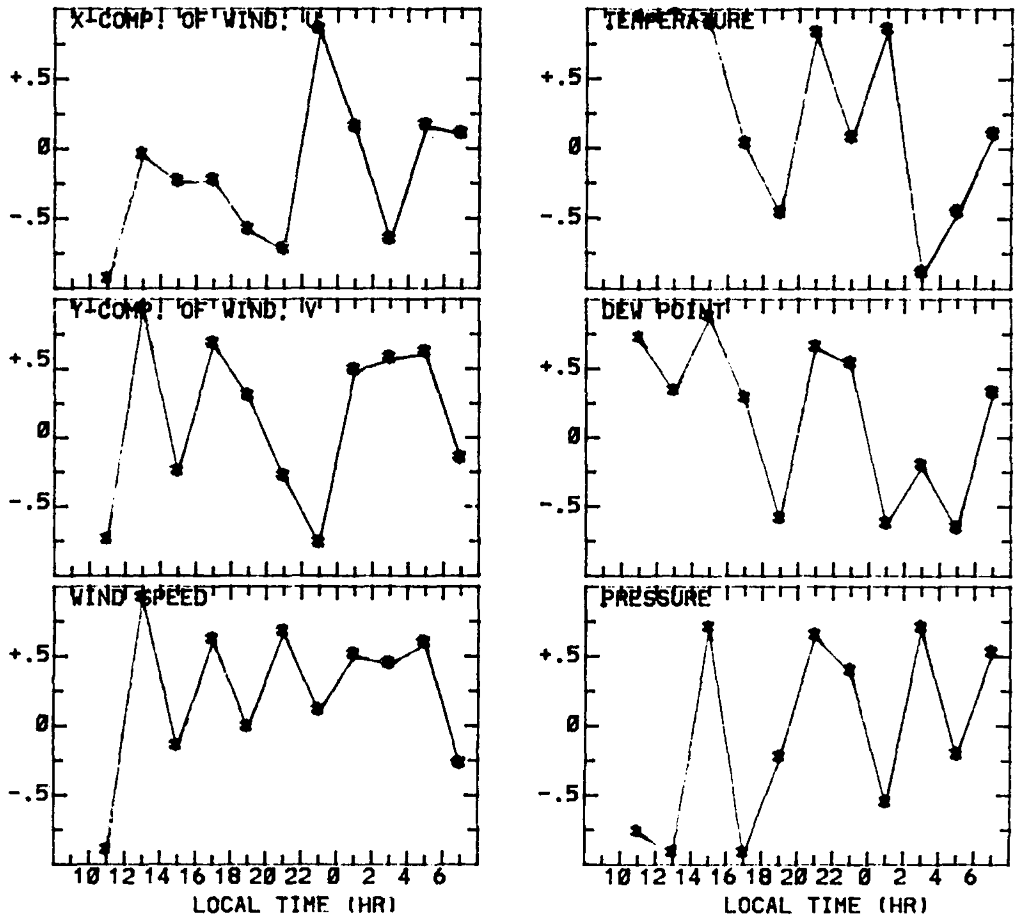

Figure 19. Time series of correlation coefficients of horizontal wind vector components, speed, temperature, dew point, and pressure for the 1000-m level.

LITERATURE CITED

Cionco, R. M., 1990, Project WIND Documentation and User Guide, Phase I: 24-hr period, 0900 PST, 27 June - 0900 hrs PST, 28 June 1985, Internal Report, U.S. Army Atmospheric Sciences Laboratory, White Sands Missile Range, NM.

Press, W. H., B. P. Flannery, S. A. Teukolsky, and W. T. Vetterling, 1989, "Numerical Recipes," The Art of Scientific Computing (FORTRAN Version), Cambridge University Press, Cambridge, MA.

Willmott, C. J., 1981, "On the Validation of Models," Physical Geography, 2:168-194.

Willmott, C. J., 1982, "Some Comments on the Evaluation of Model Performance," Bull Am Meteorol Soc, 63:1309-1313.

Willmott, C. J., S. G. Ackleston, R. E. Davis, J. J. Feddema, K. M. Klink, D. R. Legates, J. O'Donnell and C. M. Rowe, 1985, Statistics for the Evaluation and Comparison of Models, J Geophys Res, 90(C5):8995-9005.

Yamada, T., and S. Bunker, 1989, "A Numerical Model Study of Nocturnal Drainage Flows with Strong Wind and Temperature Gradients, J Appl Meteorol, 28:545-554.

DISTRIBUTION LIST FOR PUBLIC RELEASE

Commandant
U.S. Army Chemical School
ATTN: ATZN-CM-CC (S. Barnes)
Fort McClellan, AL 36205-5020

Commander
U.S. Army Aviation Center
ATTN: ATZQ-D-MA
Mr. Oliver N. Heath
Fort Rucker, AL 36362

Commander
U.S. Army Aviation Center
ATTN: ATZQ-D-MS (Mr. Donald Wagner)
Fort Rucker, AL 36362

NASA/Marshall Space Flight Center
Deputy Director
Space Science Laboratory
Atmospheric Sciences Division
ATTN: E501 (Dr. George H. Fichtl)
Huntsville, AL 35802

NASA/Marshall Space Flight Center
Atmospheric Sciences Division
ATTN: Code ED-41
Huntsville, AL 35812

Deputy Commander
U.S. Army Strategic Defense Command
ATTN: CSSD-SL-L
Dr. Julius Q. Lilly
P.O. Box 1500
Huntsville, AL 35807-3801

Commander
U.S. Army Missile Command
ATTN: AMSMI-RD-AC-AD
Donald R. Peterson
Redstone Arsenal, AL 35898-5242

Commander
U.S. Army Missile Command
ATTN: AMSMI-RD-AS-SS
Huey F. Anderson
Redstone Arsenal, AL 35898-5253

Commander
U.S. Army Missile Command
ATTN: AMSMI-RD-AS-SS
B. Williams
Redstone Arsenal, AL 35898-5253

Commander
U.S. Army Missile Command
ATTN: AMSMI-RD-DE-SE
Gordon Lill, Jr.
Redstone Arsenal, AL 35898-5245

Commander
U.S. Army Missile Command
Redstone Scientific Information Center
ATTN: AMSMI-RD-CS-R/Documents
Redstone, Arsenal, AL 35898-5253

Commander
U.S. Army Intelligence Center and Fort Huachuca
ATTN: ATSI-CDC-C (Mr. Colanto)
Fort Huachuca, AZ 85613-7000

Northrup Corporation
Electronics Systems Division
ATTN: Dr. Richard D. Tooley
2301 West 120th Street, Box 5032
Hawthorne, CA 90251-5032

Commander - Code 3331
Naval Weapons Center
ATTN: Dr. Alexis Shlanta
China Lake, CA 93555

Commander
Pacific Missile Test Center
Geophysics Division
ATTN: Code 3250-3 (R. de Violini)
Point Mugu, CA 93042-5000

Commander
Pacific Missile Test Center
Geophysics Division
ATTN: Code 3250 (Terry E. Battalino)
Point Mugu, CA 93042-5000

Lockheed Missiles & Space Co., Inc.
Kenneth R. Hardy
Org/91-01 B/255
3251 Hanover Street
Palo Alto, CA 94304

Commander
Naval Ocean Systems Center
ATTN: Code 54 (Dr. Juergen Richter)
San Diego, CA 92152-5000

Meteorologist in Charge
Kwajalein Missile Range
P.O. Box 67
APO San Francisco, CA 96555

U.S. Department of Commerce
Mountain Administration Support
Center
Library, R-51 Technical Reports
325 S. Broadway
Boulder, CO 80303

Dr. Hans J. Liebe
NTIA/ITS S 3
325 S. Broadway
Boulder, CO 80303

NCAR Library Serials
National Center for Atmos Rsch
P.O. Box 3000
Boulder, CO 80307-3000

Bureau of Reclamation
ATTN: D: 1200
P.O. Box 25007
Denver, CO 80225

HQDA
ODCSOPS
ATTN: DAMO-FDZ
Washinting, D.C. 20310-0460

Mil Asst for Env Sci Ofc of
The Undersecretary of Defense
for Rsch & Engr/R&AT/E&LS
Pentagon - Room 3D129
Washington, D.C. 20301-3080

Director
Naval Research Laboratory
ATTN: Code 4110
Dr. Lothar H. Ruhnke
Washington, D.C. 20375-5000

HQDA
DEAN-RMD/Dr. Gomez
Washington, D.C. 20314

Director
Division of Atmospheric Science
National Science Foundation
ATTN: Dr. Eugene W. Bierly
1800 G. Street, N.W.
Washington, D.C. 20550

Commander
Space & Naval Warfare System Command
ATTN: PMW-145-1G (LT Painter)
Washington, D.C. 20362-5100

Commandant
U.S. Army Infantry
ATTN: ATSH-CD-CS-OR
Dr. E. Dutoit
Fort Benning, GA 30905-5090

USAFETAC/DNE
Scott AFB, IL 62225

Air Weather Service
Technical Library - FL4414
Scott AFB, IL 62225-5458

HQAWS/DOZ
Scott AFB, IL 62225-5008

USAFETAC/DNE
ATTN: Mr. Charles Glauber
Scott AFB, IL 62225-5008

Commander
U.S. Army Combined Arms Combat
ATTN: ATZL-CAW (LTC A. Kyle)
Fort Leavenworth, KS 66027-5300

Commander
U.S. Army Combined Arms Combat
ATTN: ATZL-CDB-A (Mr. Annett)
Fort Leavenworth, KS 66027-5300

Commander
Phillips Lab
ATTN: PL/LYP (Mr. Chisholm)
Hanscom AFB, MA 01731-5000

Director
Atmospheric Sciences Division
Geophysics Directorate
Phillips Lab
ATTN: Dr. Robert A. McClatchey
Hanscom AFB, MA 01731-5000

Raytheon Company
Dr. Charles M. Sonnenschein
Equipment Division
528 Boston Post Road
Sudbury, MA 01776
Mail Stop 1K9

Director
U.S. Army Materiel Systems
Analysis Activity
ATTN: AMXSY-MP (H. Cohen)
APG, MD 21005-5071

Commander
U.S. Army Chemical Rsch,
Dev & Engr Center
ATTN: SMCCR-OPA (Ronald Pennsyle)
APG, MD 21010-5423

Commander
U.S. Army Chemical Rsch,
Dev & Engr Center
ATTN: SMCCR-RS (Mr. Joseph Vervier)
APG, MD 21010-5423

Commander
U.S. Army Chemical Rsch,
Dev & Engr Center
ATTN: SMCCR-MUC (Mr. A. Van De Wal)
APG, MD 21010-5423

Director
U.S. Army Materiel Systems
Analysis Activity
ATTN: AMXSY-AT (Mr. Fred Campbell)
APG, MD 21005-5071

Director
U.S. Army Materiel Systems
Analysis Activity
ATTN: AMXSY-CR (Robert N. Marchetti)
APG, MD 21005-5071

Director
U.S. Army Materiel Systems
Analysis Activity
ATTN: AMXSY-CS (Mr. Brad W. Bradley)
APG, MD 21005-5071

Commander
U.S. Army Laboratory Command
ATTN: AMSLC-CG
2800 Powder Mill Road
Adelphi, MD 20783-1145

Commander
Headquarters
U.S. Army Laboratory Command
ATTN: AMSLC-CT
2800 Powder Mill Road
Adelphi, MD 20783-1145

Commander
Harry Diamond Laboratories
ATTN: SLCIS-CO
2800 Powder Mill Road
Adelphi, MD 20783-1197

Director
Harry Diamond Laboratories
ATTN: SLCHD-ST-SP
Dr. Z.G. Sztankay
Adelphi, MD 20783-1197

AFMC/DOW
Wright-Patterson AFB, OH 0334-5000

National Security Agency
ATTN: W21 (Dr. Longbothum)
9800 Savage Road
Ft George G. Meade, MD 20755-6000

U. S. Army Space Technology
and Research Office
ATTN: Brenda Brathwaite
5321 Riggs Road
Gaithersburg, MD 20882

Officer in Charge
Naval Surface Weapons Center
White Oak Library
Technical Library
Silver Springs, MD 20910-1090

The Environmental Research
Institute of MI
ATTN: IRIA Library
P.O. Box 8618
Ann Arbor, MI 48107-8618

Commander
U.S. Army Research Office
ATTN: DRXRO-GS (Dr. W.A. Flood)
P.O. Box 12211
Research Trianagle Park, NC 27709

Dr. Jerry Davis
North Carolina State University
Department of Marine, Earth, &
Atmospheric Sciences
P.O. Box 8208
Raleigh, NC 27650-8208

Commander
U.S. Army Cold Regions Research
& Engineering Laboratory
ATTN: CRREL-RG (Mr. Robert Redfield)
Hanover, NH 03755-1290

Commander
U.S. Army Cold Regions Research
& Engineering Laboratory
ATTN: CECRL-RD (Dr. K.F. Sterrett)
Hanover, NH 03755-1290

Commanding Officer
U.S. Army Armament R&D Command
ATTN: DRDAR-TSS, Bldg 59
Dover, NJ 07801

U.S. Army Communications-Electronics
Command Center for EW/RSTA
ATTN: AMSEL-RD-EW-SP
Fort Monmouth, NJ 07703-5303

Commander
U.S. Army Communications-Electronics
Command
ATTN: AMSEL-EW-D (File Copy)
Fort Monmouth, NJ 07703-5303

Headquarters
U.S. Army Communications-Electronics
Command
ATTN: AMSEL-EW-MD
Fort Monmouth, NJ 07703-5303

Commander
U.S. Army Satellite Comm Agency
ATTN: DRCPM-SC-3
Fort Monmouth, NJ 07703-5303

Director
EW/RSTA Center
ATTN: AMSEL-EW-DR
Fort Monmouth, NJ 07703-5303

USACECOM
Center for EW/RSTA
ATTN: AMSEL-RD-EW-SP
Fort Monmouth, NJ 07703-5303

6585th TG (AFSC)
ATTN: RX (CPT Stein)
Holloman AFB, NM 88330

Department of the Air Force
OL/A 2nd Weather Squadron (MAC)
Holloman AFB, NM 88330-5000

PL/WE
Kirtland AFB, NM 87118-6008

Director
U.S. Army TRADOC Analysis Command
ATTN: ATRC-WSS-R
White Sands Missile Range, NM 88002

Rome Laboratory
ATTN: Technical Library RL/DOVL
Griffiss AFB, NY 13441-5700

Department of the Air Force
7th Squadron
APO, NY 09403

AWS
USAREUR/AEAWX
APO, NY 09403-5000

AF Wright Aeronautical Laboratories
Avionics Laboratory
ATTN: AFWAL/AARI (Dr. V. Chimelis)
Wright-Patterson AFB, OH 45433

Commander
U.S. Army Field Artillery School
ATTN: ATSF-F-FD (Mr. Gullion)
Fort Sill, OK 73503-5600

Commandant
U.S. Army Field Artillery School
ATTN: ATSF-TSM-TA
Mr. Charles Taylor
Fort Sill, OK 73503-5600

Commander
Naval Air Development Center
ATTN: Al Salik (Code 5012)
Warminister, PA 18974

Commander
U.S. Army Dugway Proving Ground
ATTN: STEDP-MT-DA-M
Mr. Paul Carlson
Dugway, UT 84022

Commander
U.S. Army Dugway Proving Ground
ATTN: STEDP-MT-DA-L
Dugway, UT 84022

Commander
U.S. Army Dugway Proving Ground
ATTN: STEDP-MT-M (Mr. Bowers)
Dugway, UT 84022-5000

Defense Technical Information Center
ATTN: DTIC-FDAC
Cameron Station
Alexandria, VA 22314

Commanding Officer
U.S. Army Foreign Science &
Technology Center
ATTN: CM
220 7th Street, NE
Charlottesville, VA 22901-5396

Naval Surface Weapons Center
Code G63
Dahlgren, VA 22448-5000

Commander
U.S. Army OEC
ATTN: CSTE-EFS
Park Center IV
4501 Ford Ave
Alexandria, VA 22302-1458

Commander and Director
U.S. Army Corps of Engineers
Engineer Topographics Laboratory
ATTN: ETL-GS-LB
Fort Belvoir, VA 22060

Department of the Air Force
HQ 5 Weather Wing (MAC)
ATTN: 5 WW/DN
Langley AFB, VA 23665-5000

Commander and Director
U.S. Army Corps of Engineers
Engineer Topographics Laboratory
ATTN: CEETL-ZD
Fort Belvoir, VA 22060-5546

Commander
Logistics Center
ATTN: ATCL-CE
Fort Lee, VA 23801-6000

Commander
USATRADOC
ATTN: ATCD-FA
Fort Monroe, VA 23651-5170

Science and Technology
101 Research Drive
Hampton, VA 23666-1340

Commander
U.S. Army Nuclear & Cml Agency
ATTN: MONA-ZB Bldg 2073
Springfield, VA 22150-3198